CONFERENCE PRE-PRINT

INFERNAL-KINK INSTABILITY IN NEGATIVE-TRIANGULARITY PLASAMAS WITH NEGATIVE CENTRAL SHEAR

L. Li

College of Science, Donghua University Shanghai, China Email: lili8068@dhu.edu.cn

X.M. Zhang

College of Science, Donghua University Shanghai, China

Y.O. Liu

General Atomics, PO Box 85608, San Diego, CA 92186-5608 United States of America

Z.Y. Dong

College of Science, Donghua University Shanghai, China

J.W. Li

College of Science, Donghua University Shanghai, China

Y. Liang

Forschungszentrum Julich GmbH, Association EURATOM-FZ Jülich, Institut für Energieforschung—Plasmaphysik, Trilateral Euregio Cluster, D-52425 Jülich, Germany

F.C. Zhong College of Science, Donghua University Shanghai, China

Abstract

We present a systematic numerical investigation of magnetohydrodynamic stability of the ideal infernal-kink instability in tokamak plasmas with both negative triangularity (neg-D) shaping and negative central shear for the equilibrium safety factor profile. The q-profile choice is motivated by the need to form the internal transport barrier in the neg-D plasmas, which otherwise struggle to establish an edge barrier. The calculations show that the infernal-kink mode is generally more unstable in neg-D plasmas than in their positive-triangularity (pos-D) counterparts. This is mainly due to less favourable (or even unfavourable) average magnetic curvature near the radial location of the minimum safety factor (q_{min}) as compared to the pos-D configuration. The larger Shafranov shift associated with the neg-D shape helps the mode stabilization but is not sufficient to overcome the destabilizing effect due to bad curvature. Strong poloidal mode coupling, seeded by toroidicity, elongation, triangularity, account for the slight shift with respect to that predicted by the analytic theory of the peak location of the computed mode growth versus q_{min} .

1. INTRODUCTION

The performance in the core plasma can be enhanced and the non-inductive bootstrap current can be increased due to the presence of the edge transport barrier (ETB), while simultaneously reducing the external heating power requirements, thereby improving the economy of fusion energy [1-3]. Therefore, operation in H-mode is the dominant choice for most present tokamak devices, which allows for good confinement performance and higher operating parameters [4].

However, the operation of H-mode still presents a multitude of challenges [5-7], including: (i) the strong interaction between the plasma and plasma facing components (PFCs) ascribed to the presence of the ETB; (ii) the inherent conflict between the damage limit of PFCs and the threshold for the transition between L-mode and

H-mode; (iii) intricacies in controlling detached regimes; and (iv) triggering of the so-called type-I ELMs that lead to the exhaust issues.

Recent experimental results obtained from DIII-D [8-10] and TCV [11-15], featuring negative triangularity shapes (neg-D), present a promising approach to address the aforementioned challenges associated with edge transport barrier in plasma [11, 16-19]. The absence of a strong ETB in neg-D plasms allows access to an ELM-free regime but still with good confinement [20,21]. However, further careful investigation is required to comprehend the MHD instability in these neg-D configuration plasmas.

The negative central shear (NCS) is often associated with, and facilitates the formation of, the internal transport barrier (ITB), which in turn offers one promising scenario for the advanced tokamak (AT) concept based on conventional pos-D shape [22-25]. A NCS scenario with ITB may also improve confinement in neg-D plasmas. Indeed, as plasma triangularity vanishes toward the magnetic axis, the NCS configuration may be achievable in the plasma core of neg-D discharges where shaping differences between pos-D and neg-D plasmas are minimal [26,27].

However, an equilibrium with NCS is known to be prone to the infernal, sometimes also referred to as the quasi-interchange, instability as has been frequently studied for plasmas with pos-D shapes [28-33]. This type of instability often occurs when the minimum q-value (q_{\min}) is close to a rational number, and when there is a sufficient pressure drive at the radial location of q_{\min} [19,28,34]. Onset of an infernal mode may complicate plasma operation during the current ramp-up phase (as q_{\min} evolves), or produce the so-called long-lived mode (LLM) as observed in experiments [35,36]. Furthermore, as will be reported in this work, this instability can also couple to an external kink mode in plasmas with relatively high (global) pressure, resulting in what we refer to here as the infernal-kink mode, with the associated eigenmode sharing characteristics of both the infernal and kink instabilities. The main purpose of the present work is to provide a systematic investigation of the infernal-kink instability in plasmas with NCS and with neg-D shape. For comparison, we will also consider pos-D plasmas with otherwise similar radial profiles for the equilibrium quantities, such as the safety factor and the plasma pressure.

2. RESEARCH METHODS AND EQUILIBRIUM CONSTRUCTION

The MARS-F code [37] is used to calculate the linear stability of pos-D and neg-D plasmas. This code solves the linearized resistive MHD equations in toroidal geometry and converts plasma perturbations into an eigenvalue problem. The vacuum region is modeled by solving equations $\nabla \times \mathbf{b} = 0$ and $\nabla \cdot \mathbf{b} = 0$, in the differential form, for the perturbed magnetic field \mathbf{b} . Since the Green's function approach is not utilized, the vacuum region is always finite in MARS-F. At the computational boundary, an ideal-wall boundary condition is always imposed.

Knowing roughly the onset conditions for the infernal instability, we generate a series of NCS equilibria in a semi-analytic manner as described below for the purpose of systematic investigation, for plasmas with both pos-D and neg-D shapes.

The radial profiles of the plasma equilibrium pressure P and the surface averaged toroidal current density $\langle J_{\phi} \rangle$ are analytically defined by the following formulations, which are similar to the [38]. Here, the radial profiles of P and $\langle J_{\phi} \rangle$ are specified with free parameters p_k , $k=2\sim3$ and j_k , $k=2\sim6$, respectively.

$$P(\psi_p) = H\left(1 - \frac{\psi_p}{\psi_p^{ped}}\right) \left[1 - \left(\frac{\psi_p}{\psi_p^{ped}}\right)^{p_2}\right]^{p_3} \tag{1}$$

$$\langle J_{\phi} \rangle (\psi_p) = \left(1 - \psi_p^{j_2} \right)^{j_3} + j_4 \psi_p^{j_5} \left(1 - \psi_p \right)^{j_6} \tag{2}$$

here ψ_p is the equilibrium poloidal flux, where $\psi_p = 0$ and $\psi_p = 1$ denote the location at the magnetic axis and at the plasma boundary, respectively. Another two parameters are defined as $\psi_p^{\rm ped} = 1 - \Delta$, with fixed $\Delta \equiv 0.05$. H is the Heaviside step function. In this work, the pedestal structure is not taken into account, since we focus on the infernal-kink mode with NCS structure in the centre plasma region.

The plasma boundary shape is again analytically specified, in terms of the cylindrical coordinates R and Z and with a set of free parameters b_k , $k = 1 \sim 6$,

$$R(\theta_{\rm U}) = 1 + b_1 \cos(\theta_{\rm U} + b_3 \sin(\theta_{\rm U})) \tag{3}$$

$$R(\theta_{\rm L}) = 1 + b_1 \cos(\theta_{\rm L} + b_4 \sin(\theta_{\rm L})) \tag{4}$$

$$Z(\theta) = b_1 b_2 \sin \theta - b_5 e^{(-\left|\theta + \frac{\pi}{2}\right|/b_6)^{3/2}}$$
(5)

where θ is the poloidal angle. R and Z are normalized here by the major radius R_0 associated with the geometric center of the plasma column. In order to describe the plasmas shape with the single-null-like boundary shape (associated with parameters b_5 and b_6), the plasma shape is divided into the upper and lower half-places denoted by θ_U and θ_L . The parameter b_1 defines the inverse aspect ratio of the plasma, b_2 is the elongation, b_3 and b_4 determine the triangularity of the upper and lower plasma boundary shape, respectively. In this work, we only focus on the symmetric shape, therefore, δ denotes the shape triangularity, $\delta = b_3 = b_4$.

Based on Eq. (3-5), with fixed the shape triangularity at $\delta = 0.5$ and considering the negative central magnetic field shear (the radial location of q_{\min} is at $s_{\min} = 0.6$), an equilibrium is carried out. The radial profiles of the safety factor is plotted in Fig. 1(a) and denoted by red curves, as well as the plasma boundary shape as shown in Fig. 1(b). All control parameters are summarized in Table 1.

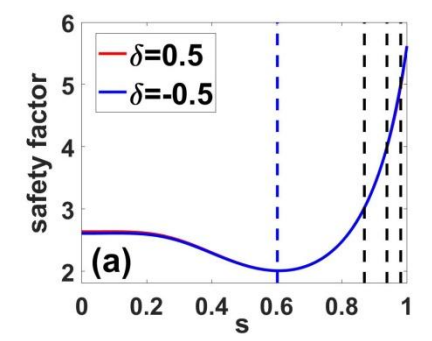
However, in order to clearly investigate the effect of the shape triangularity δ on the MHD mode stability, the whole radial profiles of the safety factor and normalized equilibrium pressure are fixed, as well as the value of $\beta_N(=2)$, with varying the shape triangularity. To achieve this, we have to introduce additional changes to the radial profile (6) for specifying the plasma toroidal current density

$$\langle f_{\phi} \rangle = \langle J_{\phi} \rangle \times \left[j_1' + j_2' \left(\left(\psi_p \right)^{1/2} - j_3' \right)^{j_4'} \left(\psi_p \right)^{j_5'/2} \right] + j_6' \psi_p \tag{6}$$

where j'_k , $k = 1 \sim 6$ are free parameters of this model. For a given radial profile of the safety factor, the radial profiles of the current are modified by specifying j'_k parameters. All parameters for several examples with varying the shape triangularity for -0.4 to 0.5 are summarized in Table 2.

The above analytic specification of the plasma boundary shape and the radial profiles for the plasma pressure and current density provides sufficient input data for numerical solution of the fixed-boundary Grad-Shafranov equation, resulting in self-consistent equilibria satisfying the MHD force balance. We referee to these as semi-analytic equilibria, which give us the basis for perform stability analysis of the infernal-kink mode reported below while varying the plasma shape.

We mentioned that a (fixed) plasma boundary, not the external equilibrium coil currents, is specified as the input to our equilibrium solver CHEASE [39]. The MARS-F stability calculations on the other hand assume the free-boundary condition and extend into the outer vacuum region.



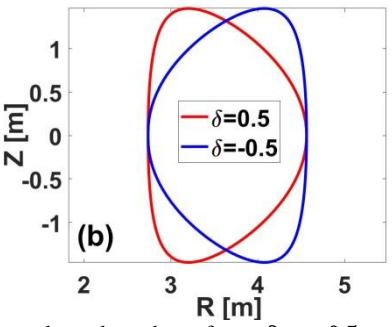


Fig 1. A series of equilibria with varying triangularity δ of the plasma boundary shape from $\delta = -0.5$ to 0.5 while fixing the safety factor profile and the $\beta_N(=2)$ value, showing (a) radial profiles of the safety factor, as well as (b) plasma boundary shapes. Here $s = (\psi_p)^{1/2}$ with ψ_p being the normalized equilibrium poloidal magnetic flux. Vertical dashed lines in (a) indicate the radial location of rational surfaces associated with the n=1 perturbation.

Table 1. Parameters p_k , j_k and b_k from Eqs. (3-5), for specifying radial profiles of the equilibrium pressure, the surface-averaged toroidal current density and the plasma boundary shape, respectively, assuming the radial location of q_{min} at $s_{qmin} = 0.6$ as shown by the red curve in Fig. 1.

# quantities	1	2	3	4	5	6
p_k		1	1.5			
j_k		1.8	2.9	65	2.22	4.85
b_k	0.25	1.6			0	1

Table 2. Parameters j'_k from Eq. (6), for specifying radial profiles of the surface-averaged toroidal current density assuming different values of the plasma boundary triangularity between -0.5 and 0.5.

$\delta = b_3 = b_4$	j_1'	j_2'	j_3'	j_4'	j_5'	j_6'
-0.5	1	0	0	0	0	0
-0.3	0.99	0.9	18	2.502	2.9	-0.033
-0.1	0.99	0.9	18	2.493	2.9	-0.022
0.1	0.99	0.9	16	2.48	2.9	0.035
0.3	1.04	0.9	16	2.48	2.8	0.133
0.5	1.0	0.9	-10	2.55	2.6	0.275

3. EFFECT OF TRIANGULARITY ON INFERNAL-KINK MODE

In this section, we focus on the n=1 toroidal mode. Because the instability that we consider here often contains external kink component, for which the wall stabilization plays a significant role, we will compare a free-boundary case without wall and a fixed-boundary case where an ideal conducting wall is placed at the plasma boundary.

First, in the no-wall boundary condition, we also fix the entire radial profile for the equilibrium safety factor (with the each radial location of q_{\min}) while varying the plasma triangularity. For example, the case as shown in Fig. 1, the radial location of q_{\min} is fixed at 0.6. The equilibrium global pressure is also fixed at $\beta_{\rm N}=2$.

Since the infernal instability - both the mode location and growth rate – also depends on the radial location of q_{\min} , we vary this parameter as well. For this purpose, a set of new equilibria (Fig. 2(a)) are generated following the same procedure as the cases shown in Fig. 1. We vary s_{\min} in a relatively large range of [0.1, 0.6] while fixing the q_{\min} value to be close to 2 (the global pressure parameter is also fixed at $\beta_{\rm N}=2$ as before). Note that for each of the q-profile shown in Fig. 2(a), we also scan the triangularity parameter from -0.5 to 0.5. For the case $q_{\min}=0.1$, is motivated by the earlier experimental results with positive triangularity and with a large central current hole [40-42]. This yields a scan of the infernal-kink stability in the 2D parameter space of (δ, s_{\min}) .

Figure 2(b) reports the MARS-F computed mode growth/damping rate in the aforementioned 2D parameter space. In general, the growth rate of the infernal-kink is non-monotonic with increasing δ at a given $s_{\rm qmin}$. A stable domain, enclosed by the black curve in Fig. 2(b), appears in this 2D parameter space, when $q_{\rm min}$ is located sufficiently further away from the magnetic axis. Note that the stable window occurs still only for pos-D shaped plasmas. The robustness of the ideal infernal-kink instability poses a MHD limitation to the neg-D scenario, if the latter is to be operated in the NCS regime.

In order to gain physics insight into the destabilization effect of the infernal-kink mode due to the neg-D shape, we consider two key equilibrium quantities associated with the shaping, that affect the low-n MHD instability. One is the Shafranov shift and the other the averaged magnetic curvature. For the infernal-kink type of mode which is partly driven by the plasma current and partly by the plasma pressure, and for equilibria with the same safety factor profile and the same global beta, the aforementioned two factors are the primary equilibrium quantities dictating the instability [43, 44].

In this work, the normalized Shafranov shift Δ/R_0 of the magnetic axis is $\Delta/R_0 = (R_{\rm axis} - R_0)/R_0$ with $R_0 = (R_{\rm max} + R_{\rm min})/2$. The Shafranov shift increases as the plasma boundary changes more towards the neg-D shape. Note again that this primarily a shaping effect since we fix the global plasma pressure. Since Shafranov shift is typically stabilizing for the MHD modes, the trend in this work does not explain the destabilization effect of the infernal-kink in neg-D plasmas.

On the other hand, in a tokamak geometry, the favorable average magnetic curvature effect is found to be stabilizing for the tearing and interchange modes [45]. The average curvature effect is often measured in terms of the Mercier Index D_R [44], which we evaluate at the q_{\min} radial location for infernal mode. Because D_R is

inversely proportional to the local magnetic shear $s_1 = (s/q)(dq/ds)$ [46], and hence approaches infinity at the q_{\min} location for an NCS equilibrium, we examine instead the asymptotic quantity s_1D_R which remains finite at the magnetic shear reversal point.

Note that a negative value of D_R implies the stabilizing effect for the tearing and interchange modes in tokamaks. In this work thus clearly quantifies the bad average curvature effect associated with the neg-D shape of the plasma, which is intuitively understandable since the equilibrium magnetic field lines tend to stay longer near the low-field side of the torus with a neg-D shape. This bad curvature effect, indicated by small negative or even positive values of s_1D_R , destabilizes the infernal-kink mode as shown in Fig. 2(b).

We point out that the eventual mode stability reported in Fig. 2(b) results from the two competing effects, i.e. the stabilization due to the Shafranov shift and destabilization due to bad curvature, as the plasma shape changes towards more neg-D shapes. This competition is also likely the reason for the stable window for the infernal-kink instability shown in Fig. 2(b), as δ becomes slightly positive.

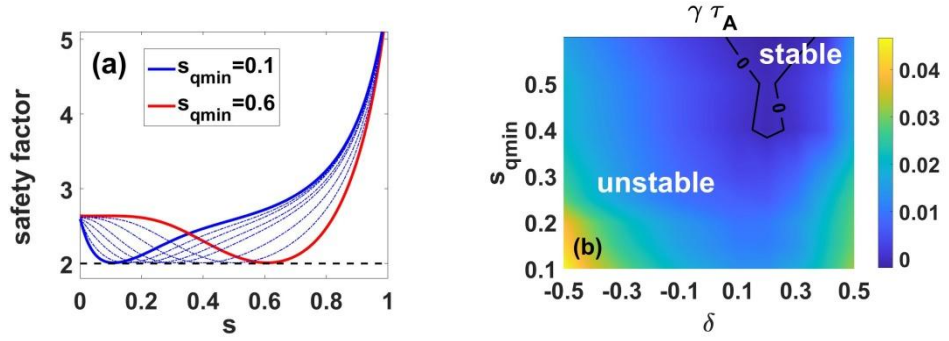


Figure 2. (a) Assumed radial profiles of the safety factor while varying the radial location $(s_{\rm qmin})$ of $q_{\rm min}$ from 0.1 to 0.6 at fixed $q_{\rm min}$ =2.01. Each safety factor profile corresponds to a series of equilibria with the plasma boundary triangularity varying from -0.5 to 0.5 as shown in Fig. 1(b). (b) The MARS-F computed growth/damping rate of the n=1 no-wall infernal-kink instability while varying both the plasma triangularity δ and the radial location $(s_{\rm qmin})$ of $q_{\rm min}$, with the safety factor profiles shown in Fig. 2(a). The black curve indicates marginal stability. The normalized plasma pressure is fixed at $\beta_{\rm N}=2$ for all equilibria in this 2D parameter scan.

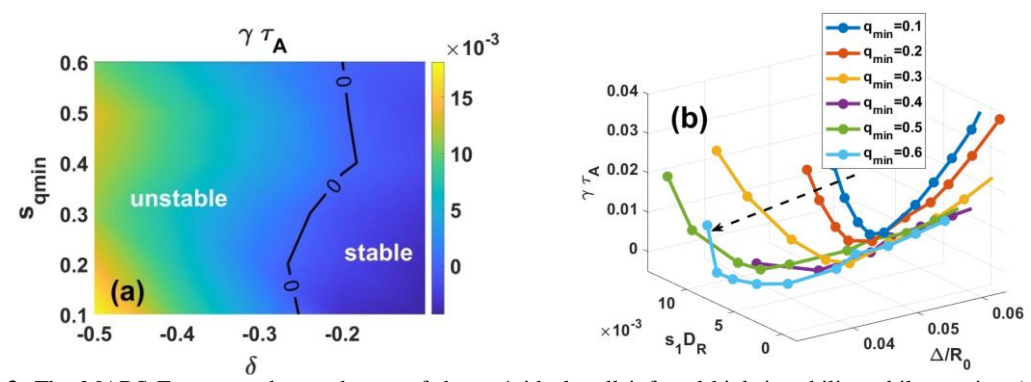


Figure 3. The MARS-F computed growth rate of the n=1 ideal-wall infernal-kink instability while varying (a) both the plasma triangularity δ and the radial location ($s_{\rm qmin}$) of $q_{\rm min}$, and (b) the corresponding parameters Δ/R_0 and s_1D_R , with the safety factor profiles shown in Fig. 4. The black curve in Fig. 9(a) indicates marginal stability of the instability. The curves in (b) correspond to varying $s_{\rm qmin}$ at fixed δ . The normalized plasma pressure is fixed at $\beta_N=2$.

The presence of large external kink components in the computed mode, based on the eigenfuncitons, complicates the stability analysis for these NCS plasmas with neg-D shape. In what follows, we try to eliminate these external kink components by placing an ideal wall at the plasma boundary, with the stability results reported in Fig. 3.

Figure 3(a) plots the MARS-F computed mode growth/damping rate in the 2-D parameter space $(\delta, s_{\text{qmin}})$, for the same sets of equilibria as in Fig. 2(b). It is evident that the ideal wall stabilization expands the stable window in the aforementioned parameter space. In particular, (i) the infernal-kink instability disappears in all plasmas with pos-D shape; (ii) more importantly, the mode becomes stable even for equilibria with relatively weak neg-D shape (δ >-0.25). Note also that (iii) the stable boundary shown in Fig. 3(a) is not very sensitive to

the radial location of q_{\min} , indicating that the plasma boundary shape (triangularity) is the main factor determining the infernal-kink stability here. Coming back to the physics discussion presented in subsection 3.2, we conclude that, in strongly shaped neg-D plasmas with NCS, the bad curvature destabilization overcomes the stabilizing influence by the Shafranov shift, with a net effect which is still destabilizing for the infernal-type of mode.

The computed mode growth rate is further quantified (Fig. 3(b)) in terms of the shafranov shift Δ/R_0 and the modified tearing index s_1D_R evaluated at $s_{\rm qmin}$, while varying the plasma boundary triangularity δ and $s_{\rm qmin}$. At fixed δ -value (and varying $s_{\rm qmin}$), the mode growth rate behaves non-monotonically as a result of simultaneous changes of Δ/R_0 and s_1D_R . The dominant contribution for this non-monotonic behavior comes from the curvature effect as indicated by D_R .

4. FURTHER IDENTIFICATION OF THE NATURE OF INSTABILITY

In what follows, we further identify the mode, by systematically investigating the influence of the q_{\min} value and plasma pressure on the mode growth rate.

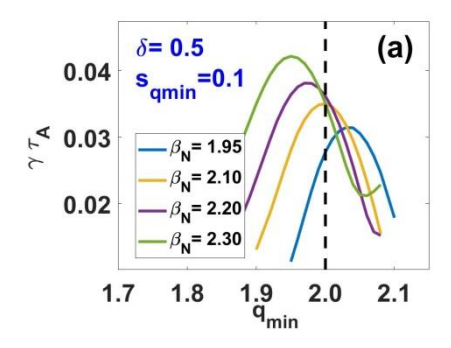
We have so far fixed the plasma pressure (at $\beta_N = 2$) and the q_{\min} value (close to 2) while studying the shaping effect (the plasma boundary triangularity). On the other hand, it is known that both proximity of q_{\min} to a rational number and the plasma pressure drive the infernal instability [43]. We will therefore vary these two parameters while fixing the triangularity. We choose two extreme cases for the latter ($\delta = -0.5$ and 0.5).

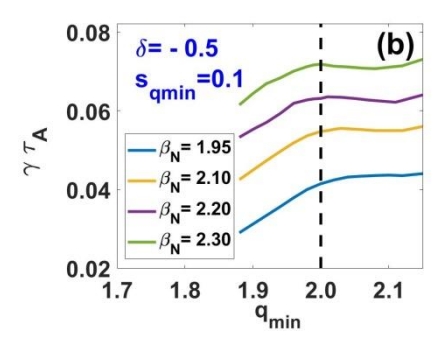
Figure 4 reports several representative results. Note that we also show two cases with different radial locations of q_{\min} , with $s_{\min} = 0.1$ and $s_{\min} = 0.6$, respectively. Several interesting observations can be made from Fig. 4.

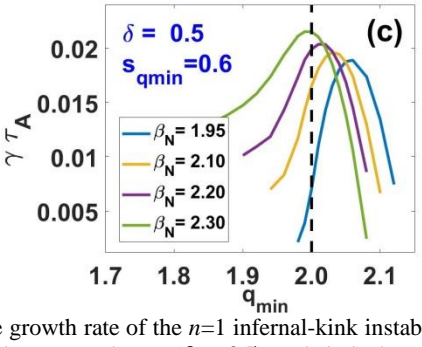
First, for the equilibria with pos-D shape ($\delta = 0.5$, Fig. 4(a, c)), the computed mode growth rate peaks near, but generally not exactly at, the integer value of $q_{\min} = 2$ (for the n=1 instability). We attribute the slight shift of the peaks from $q_{\min} = 2$, shown in Fig. 4(a,c), by the poloidal mode coupling effect as the main reason. Indeed, the relative amplitudes of the sideband (with respect to m=2) poloidal harmonics are not small. We emphasize, however, that the parabolic-like behaviour of the mode growth rate versus q_{\min} cannot be used as the sufficient condition for identifying the infernal mode.

Next, we consider cases with the neg-D shape (Fig. 3(b,d)). Here, the mode stability behaviour (versus q_{\min}) is very different between the two cases of $s_{\min} = 0.1$ and 0.6. We identify the latter as pressure-driven global kink instability. Note that this is not a simple external kink-peeling mode, since the mode remains unstable even with an ideal wall placed at the plasma boundary. The similar monotonic dependence of the growth rate on q_{\min} shows that the instability is not an infernal mode even with wall stabilization.

Our study has so far been focusing on the n=1 instability, which is most macroscopic in terms of the toroidal wavelength and is typically the most dangerous one in tokamak plasmas. On the other hand, it is well-known that high-n infernal instability also occurs, and the mode growth rate exhibits oscillations with increasing toroidal mode number [28]. Such oscillation behaviors are also recovered by MARS-F, as long as the infernal mode is the dominant component of the computed eigenfunction. One example is reported in Fig. 5, where we choose an equilibrium with $s_{\rm qmin} = 0.6$. We find that this oscillating behavior is somewhat sensitive to the choice of the q_{min} value ($q_{min} = 2.2$ in the example shown). This is not surprising given the fact that the oscillation is mainly dictated by proximity of q_{min} to rational numbers m/n for the infernal mode instability.







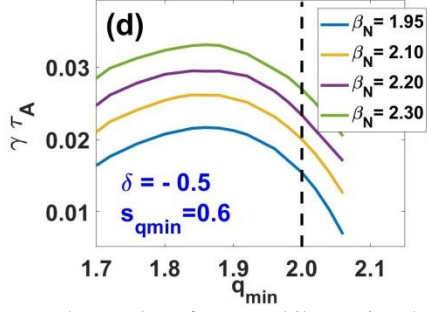
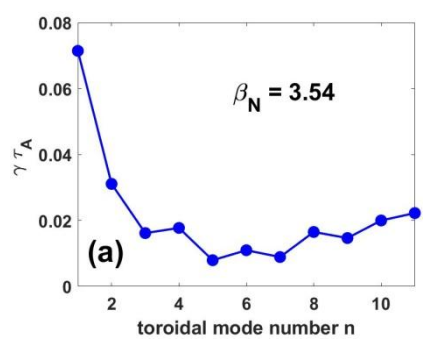


Figure 4. The growth rate of the n=1 infernal-kink instability versus the q-value of q_{\min} while varying the plasma pressure β_N , for (a,c) the pos-D shapes ($\delta=0.5$) and (b,d) the neg-D shapes ($\delta=-0.5$). In the upper and bottom panels plot the radial location of q_{\min} at $s_{\min}=0.1$ and $s_{\min}=0.6$, respectively. Here the black vertical lines denote the q-value of q_{\min} (=2).



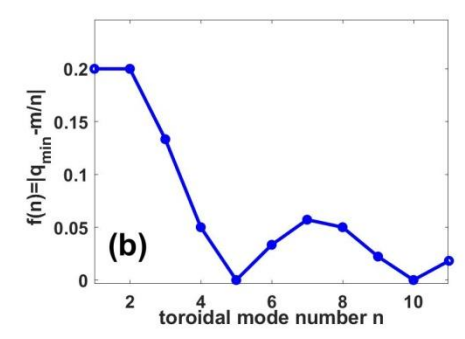


Figure 5. (a) The computed growth rate of the infernal-kink mode via MARS-F versus the toroidal mode number n, with the plasma pressure fixed at $\beta_N = 3.54$ and the radial location of q_{min} at $s_{qmin} = 0.6$. (b) The analytic function f(n) versus the toroidal mode number n, where $f(n) = \min[(q_{min} - m/n)^2]$. The value of q_{min} is fixed at $q_{min} = 2.2$.

5. CONCLUSION

We have performed numerical investigation into the stability of the n=1 ideal infernal-kink instability in neg-D plasmas with negative central shear for the equilibrium safety factor. The latter is motivated by the desire to form the internal transport barrier in the neg-D configuration, which is known to have difficulty to form the edge transport barrier. We also contrast the MHD stability results with that from the pos-D configuration, with otherwise similar equilibrium profiles (the plasma pressure, toroidal current density as well as the safety factor). All stability computations are carried out utilizing the MARS-F code, based on a series of semi-analytically designed equilibria with varying plasma boundary shape.

As a key conclusion, we find that infernal-kink mode is generally more unstable in neg-D plasmas as compared to the pos-D counterpart. This poses certain MHD limitations on achieving stable operational regime with ITB and with the neg-D concept. Based on our numerical findings, we propose a recipe for resolving this issue, by (i) forming the ITB not too close to the magnetic axis in neg-D plasmas to avoid strong kink-drive, and (ii) by allowing q_{\min} further away from rational numbers (integer numbers for the n=1 instability) to avoid the infernal drive.

For comparison, we find that the infernal-kink mode is more stable in pos-D plasmas with the same safety factor profile and the same β_N value. In fact, a stable window opens up near $\delta \sim 0.2$ for the n=1 infernal mode (with sufficient large $s_{\rm qmin}$ and without wall stabilization), as we scan triangularity of the plasma boundary shape. Imposing an ideal-wall boundary condition suppresses the external kink drive, leading to wider stable windows extending to the neg-D regime ($\delta > -0.25$).

Physics-wise, we find that the more unstable behavior of the infernal-kink mode with the neg-D configuration is mainly due to less favorable (or even unfavorable) average magnetic curvature near the $q_{\rm min}$ location, as compared to the pos-D counterpart. The larger Shafranov shift associated with the neg-D shape helps the mode stabilization, but is not sufficient to overcome the destabilizing effect due to bad curvature. On the other hand, the aforementioned two competing effects can be employed to explain the non-monotonic dependence of the computed mode growth rate versus δ and the appearance of the stable window at intermediate (positive) delta values. As another interesting physics point, we identify a strong poloidal mode

coupling due to plasma shaping (toroidicity, elongation, triangularity, etc.), which helps explain the slight shift (with respect to that predicted by the analytic theory) of the peak location of the mode growth versus q_{\min} .

6. REFERENCES

- [1] Wolf R.C. et al 2002 Plasma Phys. Control. Fusion 45 R1
- [2] Koide Y. et al 1994 Phys. Rev. Lett. 72 3662
- [3] Takenaga H. et al 2003 Nucl. Fusion 43 1235
- [4] Wagner F. et al 1982 Phys. Rev. Lett. 49 1408
- [5] Loarte A. et al 2007 Phys. Scr. 2007 222
- [6] Gunn J.P. et al 2017 Nucl. Fusion 57 046025
- [7] Kikuchi M. et al 2014 JPS Conf. Proc. 1 015014
- [8] Thome K E et al 2024 Plasma Phys. Control. Fusion 66 105018
- [9] Paz-Soldan C. et al 2024 Nucl. Fusion 64 094002
- [10] Boyes W. et al 2023 Nucl. Fusion 63 086007
- [11] Medvedev S.Yu. et al 2015 Nucl. Fusion 55 063013
- [12] Kikuchi M. *et al* 2017 Single null negative triangularity tokamak for power handling, *1st Asia-Pacific Conference on Plasma Physics* (Chengdu, China, 18-23 September 2017) (available at: MF-O13.pdf (aappsdpp.org))
- [13] Pochelon A. et al 1999 Nucl. Fusion <u>391807</u>
- [14] Coda S et al 2022 Plasma Phys. Control. Fusion 64 014004
- [15] Camenen Y. et al 2007 Nucl. Fusion 47 510
- [16] Zheng L. et al 2021 Nucl. Fusion 61 116014
- [17] Yang X. et al et al 2023 Nucl. Fusion 63 066001
- [18] Ren J. et al 2016 Plasma Phys. Control. Fusion 58 115009
- [19] Dong G.Q. et al 2017 Phys. Plasmas 24 112510
- [20] Nelson A.O. et al 2022 Nucl. Fusion <u>62 096020</u>
- [21] Yu G. et al 2023 Phys. Plasmas 30 062505
- [22] Connor J.W. et al 2004 Nucl. Fusion 44 R1
- [23] Lao L.L. et al 1996 Phys. Plasmas 3 1951–1958
- [24] Wade M.R. et al 2001 Phys. Plasmas 8 2208-2216
- [25] Leboeuf J.N. et al 2001 Phys. Plasmas 8 3358-3366
- [26] Rodr guez E. et al 2023 Journal of Plasma Physics 89(2) 05890211
- [27] Masamoto Y. et al 2022 Plasma and Fusion Research 17 2403038
- [28] Manickam J. and Pomphrey N. 1987 Nucl. Fusion 27 1461
- [29] Sato M. et al 2024 Nucl. Fusion 64 076021
- [30] Graves J.P. et al 2022 Plasma Phys. Control. Fusion 64 014001
- [31] Brunetti D. et al 2020 Plasma Phys. Control. Fusion 62 115005
- [32] Ishida Y. et al 2020 Phys. Plasmas 27 092302
- [33] Kleiner A. et al 2016 Nucl. Fusion <u>56 092007</u>
- [34] Wahlberg C. and Graves J. P., 2007 Phys. Plasmas <u>14 110703</u>
- [35] Chapman I.T. et al 2010 Nucl. Fusion <u>50 045007</u>
- [36] Deng W. et al 2014 Nucl. Fusion <u>54 013010</u>
- [37] Liu Y.Q. et al 2000 Phys. Plasmas <u>7 3681–3690</u>
- [38] Liu Y.Q. et al 2020 Plasma Phys. Control. Fusion 62 045001
- [39] Lütjens H., Bondeson A., Sauter O., 1996 Comput. Phys. Comm. 97 219
- [40] Taylor T.S., Humphreys D. A., Lao L.L., Rice B.W., and Wolf R., 1998 Bull. Am. Phys. Soc. 43 1763
- [41] Hawkes N.C., Stratton B.C., Tala T. et al 2001 Phys. Rev. Lett. 87 115001
- [42] Fujita T., Oikawa T., Suzuki T. et al 2001 Phys. Rev. Lett. 87 245001
- [43] Greene J. M. and Chance M. S. 1981 *Nucl. Fusion* 21 453
- [44] Glasser et al 1975 Phys. Fluids <u>18 875-888</u>
- [45] Glasser et al 1976 Phys. Fluids 19 567-574
- [46] Hastie R. et al 1988 Nucl. Fusion 28 585